

Toughening mechanism in a ternary polymer alloy: PBT/PC/rubber system

Masami Okamoto and Yoshihiro Shinoda

Toyobo Research Center, Toyobo Co. Ltd, Katata, Ohtsu, Shiga 520-02, Japan

and Takayuki Kojima and Takashi Inoue*

Department of Organic and Polymeric Materials, Tokyo Institute of Technology, Ookayama, Meguro-ku, Tokyo 152, Japan

(Received 9 September 1992; revised 19 January 1993)

The toughening mechanism in a ternary alloy of poly(butylene terephthalate) (PBT), polycarbonate (PC) and rubber is discussed. Transmission electron microscopy (TEM) shows that the ternary alloy has a three-phase structure; fine rubber particles covered with PC shells are dispersed in a PBT matrix. Constructing the corresponding three-phase model for analysis by the finite element method (FEM), we carried out a two-dimensional elastic-plastic analysis of the deformation mechanism. When the model was uniaxially stretched, the rubber particles induced yielding of the PC shell and the PBT matrix and the yielding zone expanded over the whole space at larger strains. This massive yielding of the plastic phases is expected to result in a large amount of energy dissipation and hence the material would be toughened. Using similar analysis of a PBT/PC/void system, the void was shown to play the same role in the toughening mechanism. As expected from the FEM analysis, the three-phase alloy exhibited ductile behaviour in the falling-dart impact test. Both tensile dilatometry and light scattering experiments suggested void formation or cavitation. TEM observation after the impact test clearly supported internal cavitation of the rubber particles. The results suggest that the ternary alloy is transformed to the PBT/PC/void system during deformation, and even after the transformation, the toughening mechanism may persist.

(Keywords: polymer blends; rubber-toughened plastic; impact strength)

INTRODUCTION

Recent types of rubber-toughened plastics, such as polyamide (PA)/rubber, poly(phenylene oxide) (PPO)/PA/rubber, polycarbonate (PC)/poly(butylene terephthalate) (PBT)/rubber and PC/PBT/ABS, are binary or ternary alloys, in which fine rubber particles are dispersed in ductile polymer matrices. Wu^{1,2} has investigated the toughening mechanism of the PA/rubber system to show that the impact energy dissipation is achieved mostly by homogeneous yielding of the PA matrix. Another toughening mechanism has been suggested for the PPO/PA/rubber system by Borggreve *et al.*³, Hobbs and Dekkers⁴ and Sue and Yee⁵. They proposed the importance of rubber cavitation; that either cavitation or void formation within the rubber particles or the interface plays an important role in the toughening process. In the light of these proposals, we carried out an elastic-plastic analysis of the deformation mechanism in a PA/rubber system using the finite element method (FEM)⁶. The rubber inclusion was found to induce yielding of the matrix around it, not only in the equatorial direction (perpendicular to the stretching direction), but also in the $\pm 45^\circ$ and $\pm 135^\circ$ directions. At larger strains, the yielded zones expanded further and eventually pervaded the whole matrix. Thus, the FEM analysis revealed a massive yielding of the matrix which results in a large amount of energy dissipation, supporting the

proposal of Wu^{1,2}. Using similar analysis on a PA/void system, the void was shown to play the same role as the rubber (although it was slightly less effective), supporting the cavitation mechanism. The results imply that, even after the rubber system is transformed to the void system by cavitation or interfacial debonding during deformation, there is still an excellent energy dissipation mechanism. In other words, the two mechanisms mentioned above are not conflicting. One problem to be discussed is the strain level at which the cavitation occurs.

In this paper, we consider the PBT/PC/rubber alloy. First, we carried out the FEM analysis to confirm the massive yielding mechanism. Then, to justify the ductile deformation even at high-speed testing, the alloy was subjected to the falling-dart impact test. Further, to observe the cavitation, we carried out tensile dilatometry, light scattering experiments and transmission electron microscopy.

EXPERIMENTAL

Materials

The PBT used in this study was a commercial product from Toyobo Co. ($\bar{M}_n = 4.7 \times 10^4$; Toyobo Plastic Division). PC was a copolymer which was kindly prepared and supplied by Mr N. Ishiai, Bayer Japan Ltd ($\bar{M}_n = 2.4 \times 10^4$). A core-shell rubber was supplied by Rohm and Haas Co. (average particle diameter = 0.2 μm). PBT, PC and the rubber were mixed using a co-rotating

* To whom correspondence should be addressed

twin screw extruder (IKEGAI Machinery Corp.; 30 mm ϕ ; $L/D=16$; barrel temperature = 300°C). The blend ratio was fixed at PBT 60/PC 25/rubber 15 by weight.

Falling-dart impact test

The falling-dart impact test was carried out on a Dymatap testing machine (General Research Co.) at room temperature. A standard ASTM D-3029 specimen (100 $\phi \times 3$ mm) was prepared by injection moulding.

Uniaxial tensile dilatometry

Using the method of Bucknall⁷, the tensile dilatometry experiment was carried out on a Tensilon 5000 testing machine at room temperature under a constant axial strain rate of 0.084 s⁻¹ using a standard ASTM D-638 specimen prepared by injection moulding. The thickness strain was assumed to be the same as the width (transverse) strain ϵ_t . The volume strain, $\Delta V/V_0$, was calculated from:

$$\Delta V/V_0 = (1 + \epsilon_a)(1 + \epsilon_t)^2 - 1 \quad (1)$$

where ΔV is the volume change, V_0 is the original volume and ϵ_a is the axial strain.

FEM analysis

To carry out the elastic-plastic analysis by the FEM, it is necessary to know the true stress-strain behaviour of the component polymers. Each polymer was injection moulded into a miniature rod-type dumb-bell specimen using the Mini-Max injection moulder (model CS-183, Custom Scientific Instruments Inc.) as described in previous papers^{8,9}. Tensile testing was carried out under a constant strain rate of 0.084 s⁻¹ at room temperature. During stretching, the diameter, D , of the specimen was observed using a video camera. After necking started, the diameter of the thinned region was assumed to be D . From the time variations of D and the load P , the true stress, σ , and the true strain, ϵ' , were calculated:

$$\sigma = P/A = 4P/\pi D^2 \quad (2)$$

$$\epsilon' = \ln \epsilon = \ln(A_0/A) = 2 \ln(D_0/D) \quad (3)$$

where A is the cross-sectional area of the specimen and the subscript 0 represents the unstretched state¹⁰. Thus the rod-type specimen provides a convenient method for estimating the variation of A with stretching by studying D .

We constructed a two-dimensional FEM model as shown in Figure 1a. Five hybrid particles with PC shell and rubber core are embedded in a PBT matrix. This three-phase model is based on a TEM observation (see Figure 10). The volume ratio of PBT/PC/rubber was set at 50/40/10. Each element was assumed to have the mechanical properties identical to those of the pure component polymer; that is, it was assumed that the element exhibits the same true stress-true strain curve observed for the component polymer. Poisson's ratio for rubber was assumed to be 0.49 and those for PBT and PC were equal to 0.37.

The FEM model was uniaxially stretched in the y direction under the plane-strain condition ($\epsilon_x = 0$). Stresses evolved in the x , y and z directions (σ_x , σ_y and σ_z) and a shear stress (τ_{xy}) were calculated for each element as a function of bulk strain. The equivalent stress $\bar{\sigma}$ defined

by:

$$\bar{\sigma} = \{1/2[(\sigma_x - \sigma_y)^2 + (\sigma_y - \sigma_z)^2 + (\sigma_z + \sigma_x)^2 + 6\tau_{xy}^2]\}^{1/2} \quad (4)$$

was also calculated, where $\bar{\sigma}$ is assumed to be a reduced tensile stress which is equivalent to the triaxial stress.

The computer program used for the FEM calculation was a two-dimensional non-linear version (EPIC-IV) which can deal with the elastic-plastic mechanics. Numerical calculations were carried out on a large-scale computer (Sun-4 Work Station, Sun-microsystem Inc.).

We also carried out a similar analysis on the PBT/PC/void system having the same geometry (Figure 1b) and compared the results with those of the PBT/PC/rubber system (Figure 1a).

Light scattering

In order to judge whether cavitation or void formation takes place during tensile deformation, we carried out the light scattering experiment using the apparatus shown in Figure 2. The intensity of scattered light I from the stretched sample was measured as a function of the

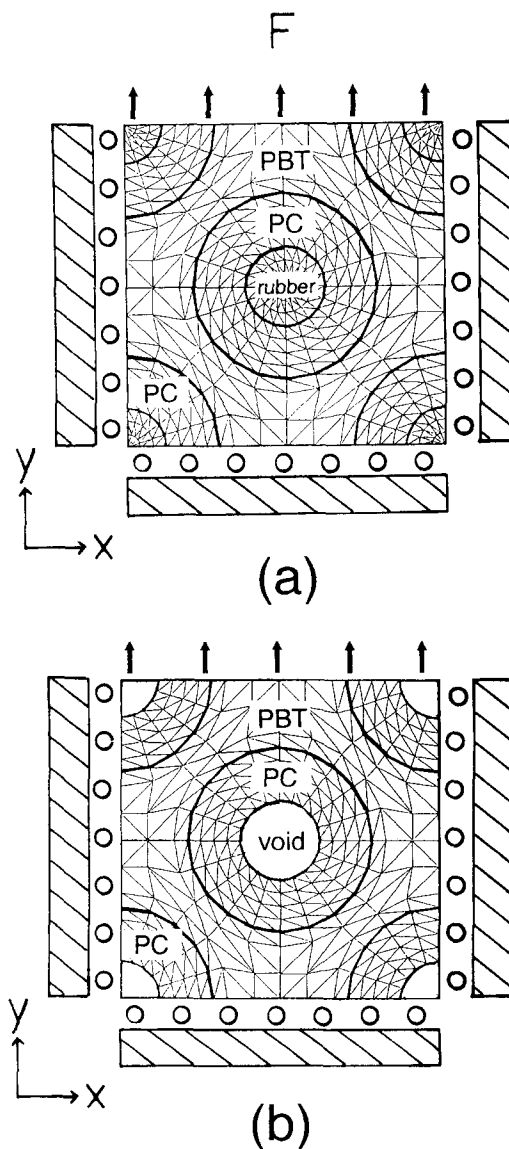


Figure 1 Two-dimensional FEM model: (a) rubber core/PC shell/PBT matrix; (b) void/PC shell/PBT matrix

scattering angle θ ($7^\circ < \theta < 38^\circ$) in the plane parallel to the stretching direction. Measurements were carried out under both Hv (vertical polarizer–horizontal analyser) and Vv (vertical–vertical) configurations. The invariant Q was calculated from

$$Q = \int_0^\infty \frac{1}{l} [I(Vv) - \frac{4}{3}I(Hv)] q^2 dq \propto \langle \eta^2 \rangle \quad (5)$$

where l is the sample thickness, q is the magnitude of the scattering vector and $\langle \eta^2 \rangle$ is the mean-square density fluctuation¹¹.

Transmission electron microscopy

After the falling-dart impact test, the specimen was stained with OsO_4 and then RuO_4 . The stained specimen was microtomed to an ultrathin section of 70 nm thickness. The phase structure in the ultrathin section was observed under an electron microscope, Hitachi H-600 (100 kV).

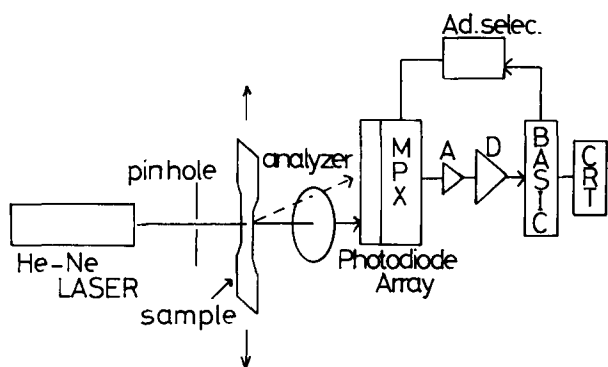


Figure 2 Light scattering photometer equipped with 46 photodiode array for the measurement of the angular dependence of scattered light intensity

RESULTS AND DISCUSSION

Figure 3 shows the true stress–true strain (σ – ϵ') curves of PBT, PC and rubber. The yield point was defined by a construction method, i.e. by drawing a tangent to the σ – ϵ' curve from a point on the ϵ' axis ($\sigma=0, \epsilon'=-1$). To simplify the FEM numerical calculation, the curve was approximated and considered to be composed of two straight lines, as demonstrated by the thin broken line for PBT in Figure 3.

Figure 4 shows typical examples of the FEM simulation. Here the von Mises criterion for yielding was applied for

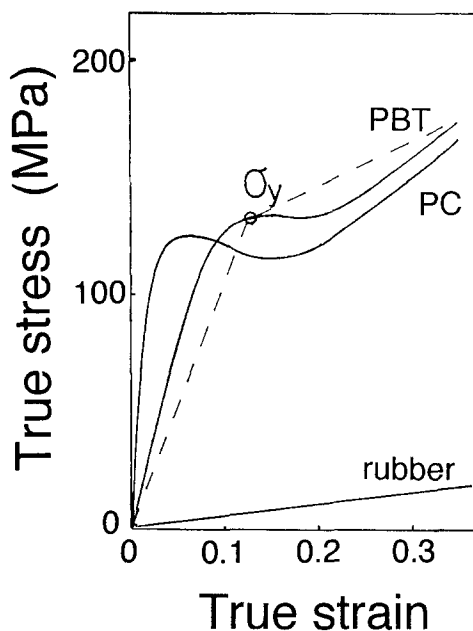


Figure 3 True stress–true strain curves of the constituent polymers and linear approximation (thin broken line)

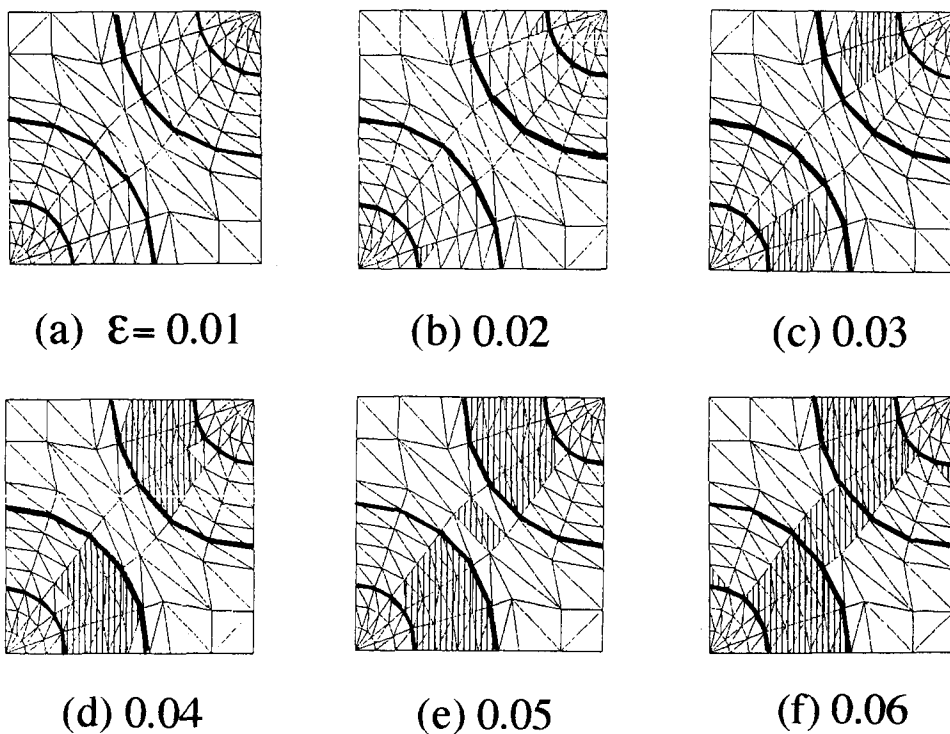


Figure 4 Deformation of the FEM model: simulation for the PBT/PC/rubber system. Yielded elements are shaded

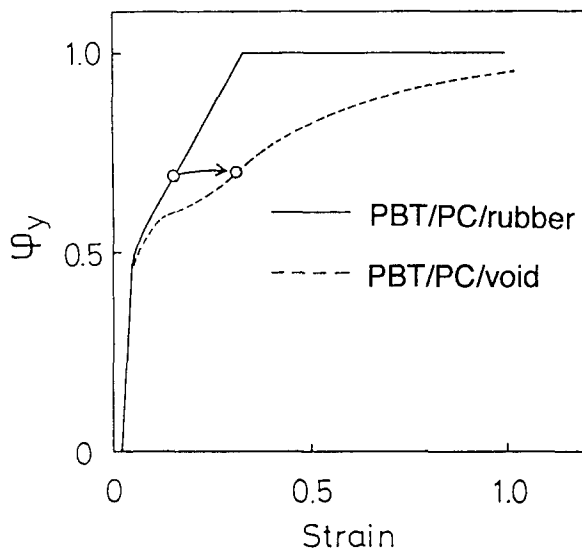


Figure 5 Variation of the number fraction of yielded elements, Ψ_y , with deformation

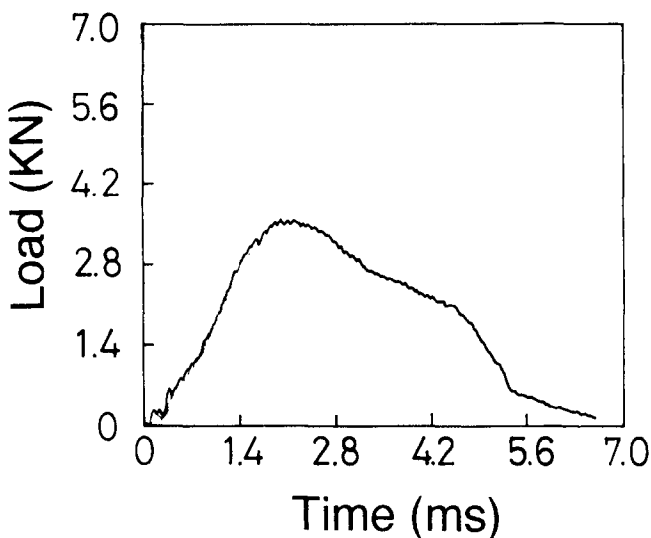


Figure 6 Load history of the falling-dart impact test for the PBT/PC/rubber 60/25/15 alloy

the FEM element, i.e. the matrix element was assumed to yield when the $\bar{\sigma}$ from equation (4) exceeded the yield stress σ_y on the σ - ϵ' curve. The elements at which $\bar{\sigma}$ are larger than σ_y are shaded. At low strain (Figure 4b), the soft (rubber) inclusion renders the stress concentration in the equatorial direction (perpendicular to the stretching direction) as expected from the linear mechanics, so that it induces yielding of the PC elements around the rubber particles. The yielded zones then expand not only in the equatorial direction but also in the $\pm 45^\circ$ directions (Figures 4c and 4d). At larger strains, the yielding pervades the PBT matrix (Figures 4e and 4f). The number fraction of yielded elements, Ψ_y , is shown as a function of bulk strain, ϵ , in Figure 5. All the matrix elements are shown to be yielded at small strain; $\Psi_y = 1$ at $\epsilon \geq 0.3$. The results seem to be essentially the same as those for the nylon/rubber system in our previous paper⁸. The similarity is to be expected, because there is a small difference in the stress-strain behaviour between PBT and PC at room temperature (as shown in Figure 2) so that the three-phase system should behave as a pseudo-

binary system consisting of rubber particles and a ductile matrix (PBT + PC).

The results in Figures 4 and 5 suggest that the massive yielding by the presence of rubber particles will result in a large amount of energy dissipation so that the pseudo-two-phase material will be toughened. Figure 5 also shows the Ψ_y - ϵ plot for the PBT/PC/void system by a broken line. It is similar to that of the rubber system (solid line) but the yielding of the matrix is slightly less massive. From a mechanical point of view, the interfacial debonding (between the rubber and the ductile plastic matrix) and/or the cavitation may correspond to a transformation from the rubber system to the void system. For instance, the transformation would be represented by the arrow in Figure 5. It should be noted that even after the switch from the course of the solid line (the rubber system) to that of the broken line (the void system), the excellent energy dissipation mechanism still exists, although it is slightly less effective than in the case of no switching. Thus, the void formation does not necessarily result in a failure in toughening, but the toughening mechanism still persists.

Figure 6 shows a load-time curve of the falling-dart impact test. The blend exhibits ductile failure, as expected from the results in Figures 5 and 6.

Figure 7 shows engineering stress-axial strain (σ - ϵ_a) and volume strain-axial strain ($\Delta V/V_0$ - ϵ_a) curves. The initial volume increase could be entirely due to elastic deformation (Poisson's effect). At intermediate strains ($2\% < \epsilon_a < 6\%$), the volume increase may be due to the shear flow and void formation. The overall volume strain can be divided into three contributions: the elastic ϵ_{ela} , the deviatoric (shear) ϵ_{dev} and the dilational (cavitation or void formation) ϵ_{dil} , assuming linear additivity¹². The strain components are given by:

$$\epsilon_{ela} = \sigma_y/E \quad (6)$$

$$\epsilon_{dil} = \Delta V/V_0 - (1 - 2\nu)\sigma_y/E \quad (7)$$

$$\epsilon_{dev} = \epsilon - \Delta V/V_0 - 2\nu\sigma_y/E \quad (8)$$

where ν is Poisson's ratio, E is Young's modulus and σ_y

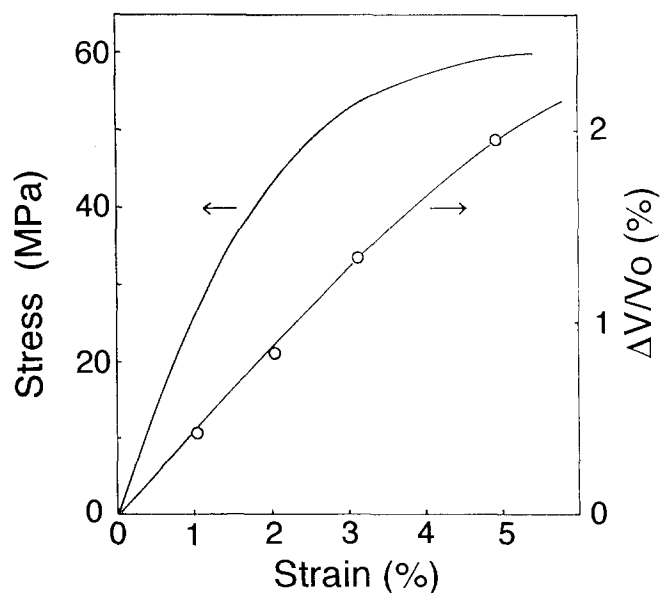


Figure 7 Stress-axial strain and volume strain-axial strain curves for the PBT/PC/rubber 60/25/15 alloy at 0.084 s^{-1}

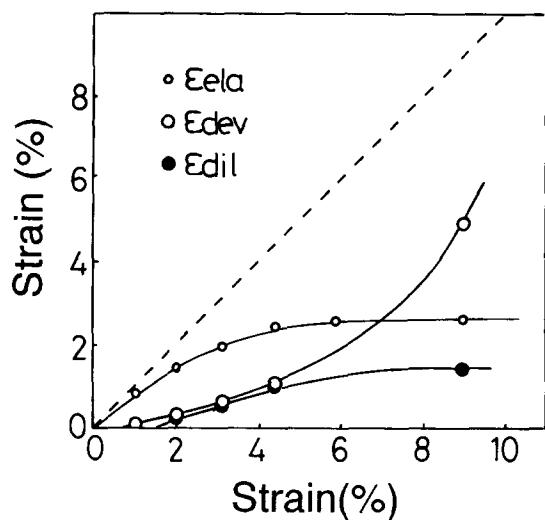


Figure 8 Elastic, deviatoric and dilational strains versus bulk strain for the PBT/PC/rubber 60/25/15 alloy

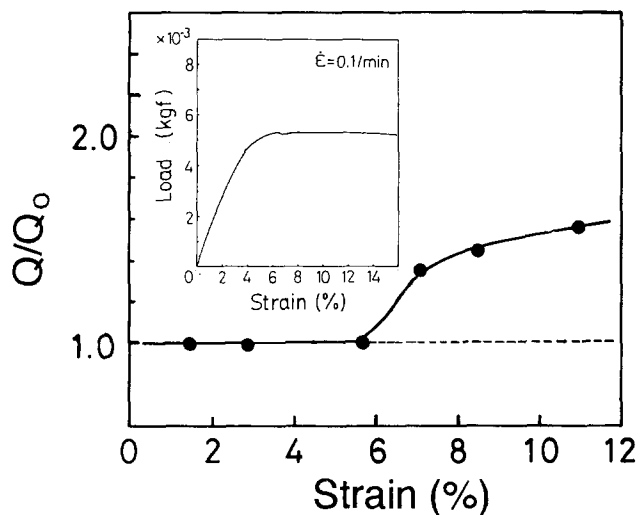


Figure 9 Light scattering invariant Q as a function of bulk strain; Q_0 for the undeformed specimen

is the yield stress. The calculated results are presented in Figure 8, which clearly shows that there are deviatoric and dilational contributions. The former starts to increase rapidly when the latter appears. However, Figure 8 shows that void formation or cavitation occurs at fairly low strain.

Figure 9 shows the change in the light scattering invariant Q ($\propto \langle \eta^2 \rangle$) with deformation. When voids are created, $\langle \eta^2 \rangle$ is expected to increase drastically, because there is a large difference in the refractive index between the void and the material. Hence an abrupt increase in Q with deformation may suggest void formation. Such an increase in Q is observed near the yield point (see small figure in Figure 9). It is at a much larger strain compared with the dilatometry analysis in Figure 8. The reason is not obvious. The thin film used for the light scattering might provide less strain constraints compared with the thick specimen used for the dilatometry.

Figure 10 shows a TEM micrograph after the falling-dart impact test. The dark region is the rubber particle stained with OsO_4 . The grey region is assigned to the PC phase stained with RuO_4 . The micrograph shows a three-phase structure; rubber particles coated

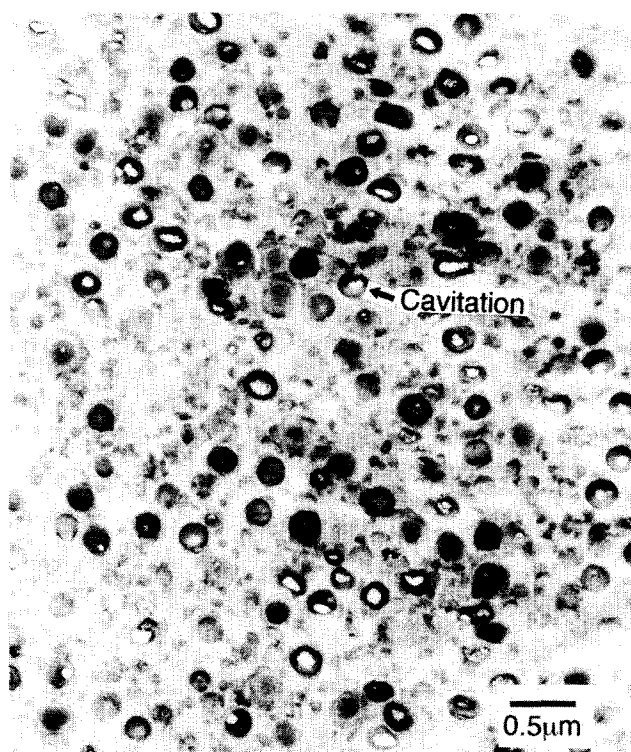


Figure 10 Transmission electron micrograph ($\text{OsO}_4/\text{RuO}_4$) of the PBT/PC/rubber 60/25/10 alloy after the falling-dart impact test. Arrow indicates a cavitation in a rubber particle

with PC shells are dispersed in a matrix of PBT. Neither craze nor debonding at the particle–matrix interface is discernible, but the cavitation in the rubber particles is clearly visible. Thus, TEM reveals the internal cavitation in the rubber particles and supports the transformation of the ductile polymer (PBT + PC)/rubber system to the ductile polymer/void system.

CONCLUSIONS

In the elastic-plastic analysis of the two-dimensional FEM, rubber inclusion was found to induce yielding of the PC shell and the PBT matrix, which would result in a large amount of energy dissipation. Ductile failure was observed in the falling-dart impact test. The ductile behaviour was consistent with the results of tensile dilatometry, which suggested a mixed mode of shear deformation and internal cavitation of the rubber particles. The cavitation was further confirmed by the light scattering experiment and TEM observation.

ACKNOWLEDGEMENTS

We thank Dr Heinz-J. Fuellmann, Bayer Japan Ltd, for helpful discussions and Mr Nobumasa Ishiai for supplying the copolycarbonate, APEC HT series.

REFERENCES

- 1 Wu, S. J. *Polym. Sci., Polym. Phys. Ed.* 1983, **21**, 699
- 2 Wu, S. *Polymer* 1985, **26**, 1855
- 3 Borggreve, R. J. M., Gaymans, R. J. and Eichenwald, H. M. *Polymer* 1989, **30**, 78
- 4 Hobbs, S. Y. and Dekkers, M. E. J. *J. Mater. Sci.* 1989, **24**, 1316
- 5 Sue, H. J. and Yee, A. F. *J. Mater. Sci.* 1991, **26**, 3449
- 6 Fukui, T., Kikuchi, Y. and Inoue, T. *Polymer* 1991, **32**, 2367

- 7 Bucknall, C. B. 'Toughened Plastics', Applied Science, London, 1977
- 8 Kikuchi, Y., Fukui, T., Okada, T. and Inoue, T. *Polym. Eng. Sci.* 1991, **31**, 1029
- 9 Fukui, T., Urabe, H. and Inoue, T. *Kobunshi Ronbunshu* 1990, **47**, 315
- 10 G'Shell, C. and Jonas, J. J. *J. Mater. Sci.* 1981, **16**, 1956
- 11 Stein, R. S. and Wilson, P. R. *J. Appl. Phys.* 1962, **33**, 1914
- 12 Heikens, D., Sjoerdsma, S. D. and Coumans, W. J. *J. Mater. Sci.* 1981, **16**, 429